Interaction-induced nonlinear magnon transport in noncentrosymmetric ferromagnets

Kosuke Fujiwara and Takahiro Morimoto
Department of Applied Physics, The University of Tokyo, Hongo, Tokyo, 113-8656, Japan
(Dated: April 5, 2024)

We study the effect of the magnon-magnon interaction on the nonlinear magnon transport. The magnon-magnon interaction induces nonreciprocal magnon decay when the time-reversal symmetry is broken, and leads to nonlinear thermal responses of magnons. We construct a theoretical framework to study the nonlinear thermal responses due to the nonreciprocal magnon decay by using the imaginary Dyson equation and quantum kinetic theory, which is then applied to a model of honeycomb ferromagnets with Dzyaloshinskii–Moriya interactions. An order estimate shows that the nonlinear thermal response from the present mechanism is feasible for experimental measurement.

Introduction.— Magnons, quasiparticles of quantized spin waves, have attracted significant attention within the field of spintronics due to their long lifetimes and capability to transmit information without Joule heating [1]. For the practical application of magnons, it is crucial to understand the transport properties of magnons. Since the magnon is a charge-neutral boson, its thermal transport has been extensively investigated [2–4], including the thermal Hall effect and the spin Nernst effect which originate from a nontrivial geometry of the magnon band [5–7].

Beyond the linear response regime, magnons also exhibit interesting nonlinear transport phenomena. For example, driving magnons with thermal gradient leads to a nonlinear spin current, known as the nonlinear spin Seebeck effect [8] and the nonlinear spin Nernst effect [9], where the latter emerges from the Berry curvature dipole of the magnon band. Application of high-intensity magnetic fields creates magnons and leads to the DC spin current generation [10–12]. Also, magnons in multiferroics generally have dipole moments and allow their excitation by electric fields of laser light, which was shown to be a geometric phenomenon related to the Berry connections in the case of collinear antiferromagnets [13]. The quantum kinetic theory gives a useful tool to analyze the nonlinear thermal transport of magnons [14–16]. In this framework, the second order nonlinear responses are divided into three parts according to their dependence on the relaxation time τ (i.e. $\propto \tau^0$, τ, and τ^2) [15]. Among them, the nonlinear Drude term, which is proportional to τ^2, is particularly important when relaxation times are long. The nonzero nonlinear Drude term requires that the magnon Hamiltonian breaks the time reversal symmetry (TRS) in addition to the inversion symmetry.

While magnons are often treated as independent particles, magnons can interact with each other, which sometimes gives drastic changes to their properties. For example, the magnon-magnon interaction modulates the band dispersion and the lifetime of magnons [17–45]. In particular, such effects on the topological magnons [26, 31, 36, 41, 42] and the associated edge modes [40, 43], strongly affect the magnitude of the thermal Hall effect [36, 41, 44, 45]. Furthermore, it was revealed that magnon-magnon interactions induce a qualitative change of quantum phases, exemplified by the interaction-

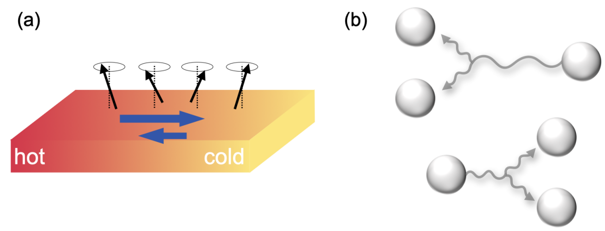

FIG. 1. The schematic picture of the nonreciprocal magnon thermal current and the nonreciprocal magnon decay. (a) Nonreciprocal thermal current (blue arrows) carried by magnon excitations (black arrows). (b) Nonreciprocal magnon decay arising from magnon-magnon interactions. Left-going and right-going magnons (white spheres) experience different decay rates due to inversion symmetry breaking.

induced topological magnons, where the magnon Hamiltonian breaks the time-reversal symmetry through the magnon-magnon interactions [36]. In this paper, we study the influence of magnon-magnon interactions on the nonlinear thermal transport of magnons, and show that the magnon-magnon interaction can induce a unique nonlinear response that cannot be captured in the independent particle picture. Specifically, the magnon-magnon interaction that breaks the TRS induces nonreciprocity in the magnon decay rate, which leads to nonlinear responses of magnons (Fig. 1). Interestingly, even when the bilinear magnon Hamiltonian effectively preserves a TRS, the magnon-magnon interaction (Fig. 1(b)) introduces breaking of the TRS and gives rise to a nonlinear Drude term. We adopt a perturbation theory and the imaginary Dyson equation to study the nonreciprocal magnon decay from the magnon-magnon interaction. This allows us to obtain the magnon lifetime and compute the nonlinear Drude terms by using the quantum kinetic theory. We apply our formalism to a model of honeycomb ferromagnets, which are experimentally relevant [46–52], and perform numerical calculations of the nonlinear thermal responses. We then estimate the effect of the nonlinear Drude term from the magnon-magnon interaction, which turns out to be comparable to that originating from an explicit TRS breaking for a free magnon Hamiltonian and is feasible for experimental measurements.

Interaction-induced nonreciprocal magnon decay.— We consider the effect of magnon-magnon interactions to the magnon damping rate. To obtain the magnon Hamiltonian, we perform the Holstein-Primakoff transformation for the spin S systems as [53]

$$\begin{aligned} S_i^+ &= \hbar\sqrt{2S - a_i^\dagger a_i}\, a_i \\ &= \hbar\sqrt{2S} a_i - \hbar a_i^\dagger a_i a_i / 2\sqrt{2S} + O(1/S\sqrt{S}), \end{aligned} \tag{1a}$$

$$\begin{aligned} S_i^- &= \hbar a_i^\dagger \sqrt{2S - a_i^\dagger a_i} \\ &= \hbar\sqrt{2S} a_i^\dagger - \hbar a_i^\dagger a_i^\dagger a_i / 2\sqrt{2S} + O(1/S\sqrt{S}), \end{aligned} \tag{1b}$$

$$S_i^z = \hbar(S - a_i^\dagger a_i), \tag{1c}$$

where $a_i^\dagger$ is a bosonic magnon creation operator at ith site, $\boldsymbol{S}_i$ is a spin operator at ith site along the spin configuration of the ground state and $S_i^\pm = S_i^x \pm iS_i^y$.

Up to the forth order of magnon operators, the magnon Hamiltonian can be written as

$$\mathcal{H} = E_0 + \mathcal{H}_2 + \mathcal{H}_3 + \mathcal{H}_4, \tag{2}$$

where E_0 is the ground state energy, H_2 is a bilinear Hamiltonian, H_3 is a cubic Hamiltonian which does not conserves magnon number, and H_4 is a quartic Hamiltonian. In collinear ferromagnetic states, by using the HP transformation and the Fourier transformation, the magnon Hamiltonians $\mathcal{H}_2$, $\mathcal{H}_3$ and $\mathcal{H}_4$ are expressed as

$$\mathcal{H}_2 = \sum_{\boldsymbol{k}} \sum_{\alpha,\beta} a_{\boldsymbol{k},\alpha}^\dagger H_{2,\boldsymbol{k}}^{\alpha,\beta} a_{\boldsymbol{k},\beta} \tag{3a}$$

$$\mathcal{H}_3 = \frac{1}{2\sqrt{N}} \sum_{\boldsymbol{k},\boldsymbol{q},\boldsymbol{p}}^{p=k+q} \sum_{\alpha,\beta,\gamma} V_{\boldsymbol{k},\boldsymbol{q},\boldsymbol{p}}^{\alpha\beta\gamma} a_{\boldsymbol{k},\alpha}^\dagger a_{\boldsymbol{q},\beta}^\dagger a_{\boldsymbol{p},\gamma} + h.c. \tag{3b}$$

$$\begin{aligned} \mathcal{H}_4 =& \frac{1}{4N} \sum_{\boldsymbol{k},\boldsymbol{q},\boldsymbol{p},\boldsymbol{l}}^{\boldsymbol{l}=\boldsymbol{k}+\boldsymbol{q}+\boldsymbol{p}} \sum_{\alpha,\beta,\gamma,\delta} W_{\boldsymbol{k},\boldsymbol{q},\boldsymbol{p},\boldsymbol{l}}^{\alpha\beta\gamma\delta} a_{\boldsymbol{k},\alpha}^\dagger a_{\boldsymbol{q},\beta}^\dagger a_{\boldsymbol{p},\gamma}^\dagger a_{\boldsymbol{l},\delta} + h.c. \\ &+ \frac{1}{4N} \sum_{\boldsymbol{k},\boldsymbol{q},\boldsymbol{p},\boldsymbol{l}}^{\boldsymbol{l}=\boldsymbol{k}+\boldsymbol{q}-\boldsymbol{p}} \sum_{\alpha,\beta,\gamma,\delta} Y_{\boldsymbol{k},\boldsymbol{q},\boldsymbol{p},\boldsymbol{l}}^{\alpha\beta\gamma\delta} a_{\boldsymbol{k},\alpha}^\dagger a_{\boldsymbol{q},\beta}^\dagger a_{\boldsymbol{p},\gamma} a_{\boldsymbol{l},\delta} + h.c., \end{aligned} \tag{3c}$$

where $a_{\boldsymbol{k},\alpha}^\dagger$ is the magnon creation operator of αth band with momentum $\boldsymbol{k}$, N is the number of unit cells, and V, W, and Y are coefficients of the magnon-magnon interactions.

We treat the magnon-magnon interaction from $\mathcal{H}_3$ and $\mathcal{H}_4$ as a perturbation to $\mathcal{H}_2$ which we incorporate as a self-energy of a magnon [22, 36, 40]. Up to the order of $1/S$, the Green's function $\mathcal{G}$ in the imaginary time formalism is given by

$$\begin{aligned} &\mathcal{G}_{k,\alpha\beta}(\tau) = \\ &\mathcal{G}_{k,\alpha\beta}^0(\tau) + \int_0^\beta d\tau_1 \langle T_\tau \mathcal{H}_4(\tau_1) a_{k,\alpha}(\tau) a_{k,\beta}^\dagger \rangle \\ &- \frac{1}{2}\int_0^\beta d\tau_1 \int_0^\beta d\tau_2 \langle T_\tau \mathcal{H}_3(\tau_1)\mathcal{H}_3(\tau_2) a_{k,\alpha}(\tau) a_{k,\beta}^\dagger \rangle, \end{aligned} \tag{4}$$

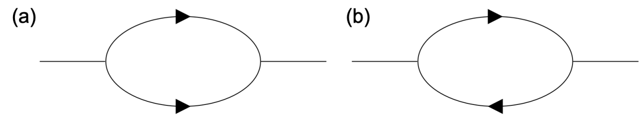

FIG. 2. Diagrams of magnon-magnon interactions which contribute to the magnon damping rate in the order of $1/S$. Bubble diagrams corresponding to (a) the first and (b) the second terms of Eq.(5). The contribution from the diagram (a) is dominant at low temperatures.

where $\mathcal{G}^0$ is the unperturbed Green function, $\beta = 1/k_B T$ is the inverse temperature, T_τ represents imaginary time ordering of operators, and $\langle \cdots \rangle$ is the thermal average for the unperturbed Hamiltonian $\mathcal{H}_2$.

The contribution of $\mathcal{H}_4$ only gives the Hartree term whose contribution is real. Consequently, it modifies the magnon energy only, leaving the magnon lifetime unchanged. The contribution of $\mathcal{H}_3$ has a two types of contribution: tadpole diagrams and bubble diagrams. While the contribution of the tadpole diagrams is real. that of the bubble diagrams shown in Fig. 2 has imaginary parts which lead to the magnon decay. Thus, we focus on the contribution of the bubble diagrams to the self energy Σ which can be written as

$$\begin{aligned} \Sigma_{\boldsymbol{k}}^{\alpha,\beta}(\omega,T) = \frac{1}{N}\sum_q \sum_{\gamma,\gamma'} \Bigg(&\frac{1}{2} \frac{V_{\boldsymbol{q},\boldsymbol{k}-\boldsymbol{q},\boldsymbol{k}}^{\gamma,\gamma',\beta} (V_{\boldsymbol{q},\boldsymbol{k}-\boldsymbol{q},\boldsymbol{k}}^{\gamma,\gamma',\alpha})^*}{\omega - \varepsilon_{\boldsymbol{q},\gamma} - \varepsilon_{\boldsymbol{k}-\boldsymbol{q},\gamma'} + i\eta} \\ &\times [f_{\boldsymbol{q},\gamma,T}^B + f_{\boldsymbol{k}-\boldsymbol{q},\gamma',T}^B + 1] \\ &+ \frac{(V_{\boldsymbol{k},\boldsymbol{q},\boldsymbol{k}+\boldsymbol{q}}^{\beta,\gamma,\gamma'})^* V_{\boldsymbol{k},\boldsymbol{q},\boldsymbol{k}+\boldsymbol{q}}^{\alpha\gamma,\gamma'}}{\omega + \varepsilon_{\boldsymbol{q},\gamma} - \varepsilon_{\boldsymbol{k}+\boldsymbol{q},\gamma'} + i\eta} \\ &\times [f_{\boldsymbol{q},\gamma,T}^B - f_{\boldsymbol{k}+\boldsymbol{q},\gamma',T}^B] \Bigg). \end{aligned} \tag{5}$$

Here, $\varepsilon_{\boldsymbol{k},\gamma}$ is a magnon energy of the band γ determined by $\mathcal{H}_2$ and $f_{\boldsymbol{k},\gamma,T}^B = 1/(\exp(\beta\varepsilon_{\boldsymbol{k},\gamma}) - 1)$ is a Bose distribution function. The first and second terms correspond to contributions from Fig. 2(a) and Fig. 2(b), respectively. In particular, at the zero temperature, only the first term from Fig. 2(a) is nonzero and the second term from Fig. 2(b) vanishes, indicating that the first term (particle-particle diagram) gives a dominant contribution at low temperatures.

The non-reciprocity of the self-energy is encoded in the difference of the self energy at the opposite momenta k and $-k$. By comparing $\Sigma_{\boldsymbol{k}}^{\alpha,\beta}(\omega,T)$ and $\Sigma_{-\boldsymbol{k}}^{\alpha,\beta}(\omega,T)$ (which is obtained by substituting $\boldsymbol{k}$ to $-\boldsymbol{k}$ and $\boldsymbol{q}$ to $-\boldsymbol{q}$ in Eq. (5)) and assuming $\varepsilon_{\boldsymbol{k}} = \varepsilon_{-\boldsymbol{k}}$ due to the TRS for the bilinear magnon Hamiltonian $H_{2,\boldsymbol{k}}$, we finds that the nonreciprocity in the self energy $\Sigma_{\boldsymbol{k}}^{\alpha,\beta}(\omega,T) \neq \Sigma_{-\boldsymbol{k}}^{\alpha,\beta}(\omega,T)$ requires the condition $V_{\boldsymbol{k},\boldsymbol{q},\boldsymbol{p}}^{\alpha,\gamma,\gamma'}(V_{\boldsymbol{k},\boldsymbol{q},\boldsymbol{p}}^{\beta,\gamma,\gamma'})^* \neq V_{-\boldsymbol{k},-\boldsymbol{q},-\boldsymbol{p}}^{\alpha,\gamma,\gamma'}(V_{-\boldsymbol{k},-\boldsymbol{q},-\boldsymbol{p}}^{\beta,\gamma,\gamma'})^*$. This condition is generally met for magnon-magnon interactions with broken TRS.

Now we focus on the magnon damping caused within each magnon band and ignore the off-diagonal part of

Σ. We introduce the damping rate Γ induced by the magnon-magnon interaction as the imaginary part of the self-energy

$$\Gamma_{\boldsymbol{k}}^{\alpha}(\omega,T) = -\mathrm{Im}\Sigma_{\boldsymbol{k}}^{\alpha,\alpha}(\omega,T). \tag{6}$$

To compute the nonlinear thermal conductivity, we use the Born approximation, which replaces ω in the right hand of Eq. (6) with $\varepsilon_{\boldsymbol{k},\alpha}$, but this sometimes causes an unphysical divergence. To avoid such divergence, we adopt imaginary Dyson equation [22, 26, 40] at a finite temperature, in which we solve the self-consistent equation

$$\tilde{\omega} = \varepsilon_{\boldsymbol{k}} - i\Gamma_{\boldsymbol{k}}(\tilde{\omega}^*,T), \tag{7}$$

where $\tilde{\omega}^*$ denotes a complex conjugate of $\tilde{\omega}$, which originates from the causality. We approximate $\Gamma_{\boldsymbol{k}}(\omega,T)$ in Green's functions by $\Gamma_{\boldsymbol{k}}(\tilde{\omega},T)$ and obtain the magnon damping $\Gamma_{\boldsymbol{k}}(\tilde{\omega},T)$ by solving Eq. (6) and Eq. (7) self-consistently. The magnon damping $\Gamma_{\boldsymbol{k}}(\tilde{\omega},T)$ shows an enhancement when the magnon dispersion $\varepsilon_{\boldsymbol{k}}$ overlaps with two-magnon continuum $\varepsilon_{\boldsymbol{q}} + \varepsilon_{\boldsymbol{k}-\boldsymbol{q}}$ or the collision continuum $\varepsilon_{\boldsymbol{q}} - \varepsilon_{\boldsymbol{k}+\boldsymbol{q}}$, since the numerators in Eq. ((5)) are real for $\alpha = \beta$ and the denominators become purely imaginary. In particular, the two-magnon continuum becomes important at low temperatures because the first term of Eq. (5) is nonzero even at zero temperature. In contrast, the collision becomes unimportant at low temperatures because the second term in Eq. (5) vanishes at zero temperature. If we write the magnon damping due to effects other than the magnon-magnon interaction (e.g. impurity scattering and interactions with phonons) by η, the magnon lifetime of the γth band $\tau_{\boldsymbol{k},\gamma}$ can be expressed as $\tau_{\boldsymbol{k},\gamma} = 1/2(\eta_{\boldsymbol{k},\gamma} + \Gamma_{\boldsymbol{k}}^{\gamma}(\tilde{\omega},T))$. Hereafter, we assume that $\eta_{\boldsymbol{k},\gamma} = 2\alpha\varepsilon_{\boldsymbol{k},\gamma}$ where α is a damping factor. This assumption corresponds to the phenomenological Gilbert damping.

Nonlinear thermal current of magnons.— Now we consider the nonlinear thermal current generated by the thermal gradient

$$J_Q^{\mu} = \sigma^{\mu\nu\nu}(\partial_\nu T)^2. \tag{8}$$

From the quantum kinetic theory, the nonlinear Drude term is written as [15]

$$\sigma_{nd}^{\mu\nu\nu} = \sum_n \int \frac{dk^3}{(2\pi)^3}\left[-\frac{1}{\hbar T}\tau_{\boldsymbol{k},\gamma}^2\varepsilon_{\boldsymbol{k},\gamma}^2 v_{\boldsymbol{k},\gamma}^{\mu}\frac{\partial v_{\boldsymbol{k},\gamma}^{\nu}}{\partial k_\nu}\frac{\partial f_{\boldsymbol{k},\gamma}^{B}}{\partial T} + \tau_{\boldsymbol{k},\gamma}^2\varepsilon_{\boldsymbol{k},\gamma}v_{\boldsymbol{k},\gamma}^{\mu}(v_{\boldsymbol{k},\gamma}^{\nu})^2\frac{\partial^2 f_{\boldsymbol{k},\gamma}^{B}}{\partial^2 T}\right], \tag{9}$$

where $v_{\boldsymbol{k},\gamma}^{\mu} = \partial_{k_\mu}\varepsilon_{\boldsymbol{k},\gamma}/\hbar$ is the group velocity of magnons in the γth band. If there is the TRS, $\varepsilon_{\boldsymbol{k},\gamma} = \varepsilon_{-\boldsymbol{k},\gamma}$, $\boldsymbol{v}_{\boldsymbol{k},\gamma} = -\boldsymbol{v}_{-\boldsymbol{k},\gamma}$, $\tau_{\boldsymbol{k},\gamma} = \tau_{-\boldsymbol{k},\gamma}$, the nonlinear Drude term vanishes. Thus, the nonzero nonlinear Drude term requires not only broken inversion symmetry but also broken TRS.

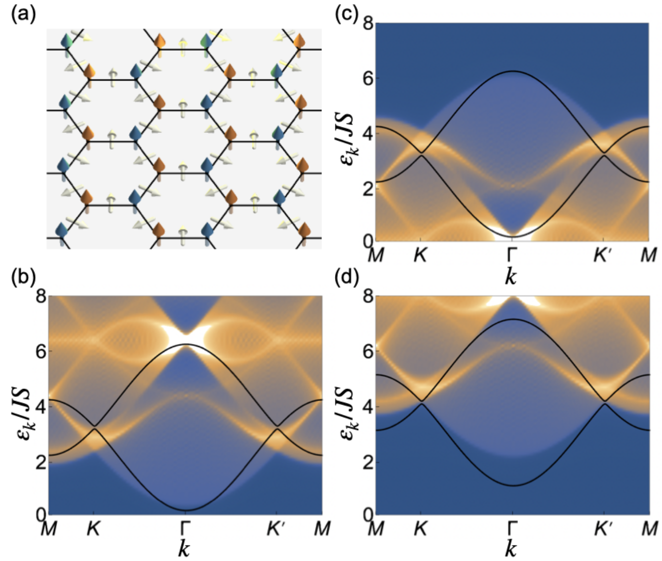

FIG. 3. The schematic picture of the spin model and the associated band dispersion. (a) The honeycomb lattice ferromagnets with DMI. Orange and green arrows represent spin moments and gray arrows represent DMI between the neighboring spins. (b-d) The magnon band dispersion (black curves) with D_{two} ((b) and (d)) and D_{coll} (c) (color plot) along high-symmetry paths of the Brillouin zone. $\Delta_A/J = 0.0$, $\Delta_B/J = 0.05$, $\mu_A = \mu_B = 1.0$, $S = 1$ and $h/JS = 0.1$ for (b) and (c) and $h/JS = 1.0$ for (d).

Application to honeycomb ferromagnets.— To demonstrate nonlinear thermal current due to the nonreciprocal magnon decay, we consider the spin model of two-dimensional ferromagnets on the honeycomb lattice as depicted in Fig. 3 (a). The spin Hamiltonian is given by

$$H = -\frac{J}{2}\sum_{\langle i,j\rangle}\boldsymbol{S}_i\cdot\boldsymbol{S}_j + \frac{D}{2}\sum_{\langle i,j\rangle}\boldsymbol{d}\cdot\boldsymbol{S}_i\times\boldsymbol{S}_j - h\sum_i g_\alpha S_i^z - \sum_i \Delta_\alpha (S_i^z)^2, \tag{10}$$

where $\boldsymbol{d}_{ij} = \boldsymbol{z}\times(\boldsymbol{r}_j - \boldsymbol{r}_i)/|\boldsymbol{r}_j - \boldsymbol{r}_i|$, and g_α is the g factor for the spins on α ($\alpha = A, B$) sites and Δ_α is the magnetic anisotropy for α sites. Here, we consider the symmetry of the spin Hamiltonian. In ferromagnets, the spin configuration breaks the TRS because the time-reversal flips spins. However, there still exists an effective TRS, composed of time-reversal and rotation in spin space, in the absence of the Dzyaloshinskii–Moriya interaction (DMI) ($D = 0$)[36]. This model also possesses an effective inversion-symmetry, consisting of inversion and rotation in spin space, in the absence of the magnetic anisotropy difference ($\Delta_A = \Delta_B$). Therefore, a nonzero nonlinear Drude term requires $D \neq 0$ and $\Delta_A \neq \Delta_B$ by breaking both effective TRS and inversion symmetry. Moreover, this honeycomb magnet model has a C_3 rotation symmetry and the symmetry IM_x composed of inversion symmetry and mirror symmetry along the yz-plane. Due to the C_3 rotation symmetry the nonlinear

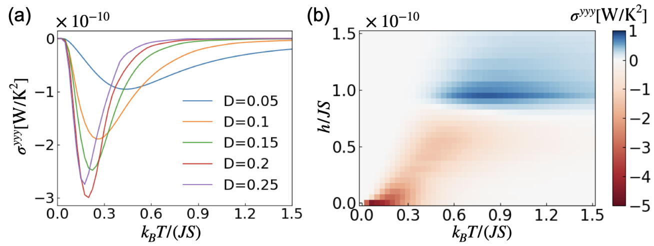

FIG. 4. Nonlinear thermal conductivity σ^{yyy} induced by the nonreciprocal magnon decay. (a) Temperature dependence of σ^{yyy} for different values of the DMI. (b) The color plot of σ^{yyy}. σ^{yyy} shows a sign change around $h/JS = 1.0$. We used the following parameters: $\Delta_A/J = 0.0$, $\Delta_B/J = 0.05$, $\mu_A = \mu_B = 1.0$, $S = 1$ and $\alpha = 0.001$. We used $h/JS = 0.1$ for (a), $D/J = 0.15$ for (b).

Hall current due to the Berry curvature dipole ($\propto \tau$) vanishes [54], and the nonlinear thermal responses satisfies $\sigma^{yyy} = -\sigma^{yxx}$ and $\sigma^{xxx} = -\sigma^{xyy}$. Also, the symmetry IM_x leads to $\sigma^{xxx} = 0$. Therefore, the nonlinear thermal response in this model arises from the nonlinear Drude term and satisfies $\sigma^{yyy} = -\sigma^{yxx}$ and $\sigma^{xxx} = \sigma^{xyy} = 0$.

The bilinear magnon Hamiltonian $H_{2,\boldsymbol{k}}$ for Eq. (10) is written as

$$H_{2,\boldsymbol{k}} = \begin{pmatrix} 3JS + hg_A + 2S\Delta_A & -JS\gamma_{\boldsymbol{k}} \\ -JS\gamma_{-\boldsymbol{k}} & 3JS + hg_B + 2S\Delta_B \end{pmatrix}, \tag{11}$$

with $\gamma_{\boldsymbol{k}} = \sum_{j=1}^{3} e^{i\boldsymbol{k}\cdot\boldsymbol{\delta}_j}$, where δ_j are the vectors pointing from one site to three neighboring sites. We show the magnon band dispersion and the two-magnon density of states $D_{two}(\omega) = \frac{1}{N}\sum_{\gamma,\gamma'}\sum_{\boldsymbol{q}\in BZ}\delta(\omega - \varepsilon_{\boldsymbol{q},\gamma} - \varepsilon_{\boldsymbol{k}-\boldsymbol{q},\gamma'})$ in Fig. 3(b) and (d) and the magnon band dispersion and the collision density of states $D_{coll}(\omega) = \frac{1}{N}\sum_{\gamma,\gamma'}\sum_{\boldsymbol{q}\in BZ}\delta(\omega - \varepsilon_{\boldsymbol{q},\gamma} + \varepsilon_{\boldsymbol{k}+\boldsymbol{q},\gamma'})$ in Fig. 3(c). As we mentioned before, when the magnon dispersion $\varepsilon_{\boldsymbol{k}}$ overlaps with the region of large D_{two} and D_{coll}, the magnon-magnon interaction has a significant effect on the magnon lifetime. Now, we incorporate the effect of the H_3 that breaks the effective TRS as a magnon damping by solving Eq. (7). An explicit expression for H_3 is given in Appendix A. By using Eq. (9), we obtain the nonlinear Drude term as shown in Fig. 4.

Figure 4 (a) shows the nonlinear thermal conductivity σ^{yyy} for five values of the DMI. The peak of σ^{yyy} shifts to lower temperatures as the DMI increases. This behavior can be explained from the two-magnon continuum and the collision continuum. From Fig. 3(b), we can see that at low energies, the overlap between $\varepsilon_{\boldsymbol{k}}$ and the two-magnon continuum is small. Thus, when the DMI is small and H_3 is small, the contribution of the first term in Eq. (5) to $\Gamma_{\boldsymbol{k}}$ is small. While the magnon dispersion $\varepsilon_{\boldsymbol{k}}$ shows a significant overlap with the collision continuum at low energy, as shown in the Fig. 3(c), the contribution of the second term in Eq. (5) to $\Gamma_{\boldsymbol{k}}$ is small at low temperatures as we mentioned before. Thus, when the DMI is small, σ^{yyy} has a peak at high temperatures. On the other hand, as the DMI increases, the contribution of the first term in Eq. (5) to $\Gamma_{\boldsymbol{k}}$ increases even if the overlap between $\varepsilon_{\boldsymbol{k}}$ and the two-magnon continuum is not so large. This results in the shift of the peak of σ^{yyy} toward lower temperatures, as the DMI increases. Furthermore, up to $D/J \sim 0.2$, the magnitude of σ^{yyy} increases as the DMI increases, but above $D/J \sim 0.2$, the magnitude of σ^{yyy} decreases as the DMI increases (Fig. 4(a)). Specifically, the nonreciprocity in the magnon decay increases for larger DMI, whereas, for too large DMI, the lifetime of magnons becomes short and the nonlinear response proportional to τ^2 is suppressed.

Figure 4 (b) shows the magnetic field and the temperature dependence of the nonlinear thermal conductivity σ^{yyy}. As the magnetic field increases, the response appears at the higher temperature, and furthermore the sign of the response changes around $h/JS \sim 1$. This behaviour can be explained by the energy shift and overlap between the magnon energy $\varepsilon_{\boldsymbol{k}}$ and the two-magnon continuum or the collision continuum. Due to the magnetic field, the magnon band dispersion shifts to higher energy. In particular, if $\mu_A = \mu_B = \mu$, magnon energy shifts by μh, while the two-magnon continuum shifts by $2\mu h$. In particular, in the range $h/JS > 1$, only the upper magnon band overlaps with the two-magnon continuum as shown in Fig. 3(d). Since the sign of magnon group velocity $\boldsymbol{v}_{\boldsymbol{k}}$ are opposite between the lower and upper bands, the sign of the nonlinear thermal conductivity changes around $h/JS \simeq 1$. Since the collision continuum is independent of the magnetic field, an overlap of magnon energy with collision continuum becomes very small for large magnetic fields, resulting in less contribution to the nonlinear conductivity. In general, as the magnetic field is increased, the overlap between the magnon energy and the two-magnon continuum and collision continuum becomes smaller and the effect of magnon-magnon interaction becomes smaller.

Discussion.— Let us estimate the order of magnitude of the nonlinear thermal current induced by the magnon-magnon interaction. Assuming that the lattice constant is 5 and the interlayer distance is 10 Å, we obtain the nonlinear thermal conductivity of $\sigma \simeq 5 \times 10^{-10}$ W/K^2 from Fig. 4(b). For the temperature gradient $\nabla T \simeq 10^5$ K/m, the nonlinear thermal current of $J_Q \simeq 5$ W/m^2. In particular, the nonlinear Hall thermal current from σ^{yxx} is feasible for experimental measurements. Since the typical value of linear thermal Hall conductivity is given by $\kappa_{xy} \simeq 10^{-4} \sim 10^{-3}$ W/Km [3, 55, 56], the linear contribution gives $J_Q \simeq 10 \sim 100$ W/m^2 for the temperature gradient $\nabla T \simeq 10^5$ K/m. Therefore, the nonlinear contribution to the thermal Hall current from σ^{yxx} is sizable compared to the linear contribution from κ_{xy}.

In this study, we adopted the spin model which gives the harmonic magnon Hamiltonian H_2 with the effective TRS, while the magnon-magnon interaction breaks the effective TRS and induces the nonreciprocal magnon damping and the nonlinear responses. In general models,

H_2 can also break the effective TRS (which we refer to here as the "explicitly broken TRS") and induce a nonlinear response within the harmonic theory. Let us compare the magnitudes of the nonlinear responses induced by the magnon-magnon interaction and the "explicitly broken TRS". Here, we consider a model where the DM vector is oriented in the z direction and H_2 does not have the effective TRS in a similar way to the Haldane model. In this "explicitly broken TRS" model, we obtain $\sigma^{\mu\nu\nu}$ of the order of 10^{-10} W/K^2 which is the same order with the nonlinear thermal conductivity induced by the magnon-magnon interaction (for details see Appendix B), indicating that the effect of the magnon-magnon interaction is not negligible even in cases with the explicitly broken TRS. In addition, the non-reciprocity from these two mechanisms shows qualitatively different behaviors with respect to the DMI D. The lifetime of the magnon incorporating the magnon-magnon interaction is written as

$$\begin{aligned}\tau_{\boldsymbol{k},D} &= 1/(\alpha\varepsilon_{\boldsymbol{k}} + \Gamma_{\boldsymbol{k}}) \sim 1/(\alpha\varepsilon_{\boldsymbol{k}} + c_1\varepsilon_{\boldsymbol{k}} D^2/J^2) \\ &\sim \tau_{\boldsymbol{k},D=0}(1 - c_1 D^2/J^2\alpha), \end{aligned} \tag{12}$$

whereas that for explicitly broken TRS systems without the magnon-magnon interaction is

$$\begin{aligned}\tau_{\boldsymbol{k},D} &= 1/(\alpha\varepsilon_{\boldsymbol{k},D}) \sim 1/\alpha\varepsilon_{\boldsymbol{k},D=0}(1 + c_2 D/J) \\ &\sim \tau_{\boldsymbol{k},D=0}(1 - c_2 D/J). \end{aligned} \tag{13}$$

Here, c_1 and c_2 are coefficients of order of unity. Therefore, if D/J is larger than α, the non-reciprocity induced by the magnon-magnon interaction becomes important compared to that induced by the "explicitly broken TRS". Furthermore, the perpendicular DMI that breaks the effective TRS of H_2 arises from spin-orbit coupling, while the in-plane DMI originates from the crystal structure. Therefore, the in-plane DMI can be larger than the perpendicular DMI, where the magnon-magnon interaction can contribute more significantly to the nonlinear thermal response.

The multiferroic kamiokite materials $M_2Mo_3O_8$ (M:3d transition metal) [55, 57] can be the candidate material for the magnon-magnon interaction induced nonlinear responses. One may also consider a heterostructure of honeycomb ferromagnets CrI_3 or $CrBr_3$ [47, 48] on top of a substrate to introduce inversion symmetry breaking to the system. While we considered the in-plane DMI as the origin of the magnon-magnon interaction, the Kitaev-Γ model [58–60] also gives rise to the magnon-magnon interactions and application of our theory leads to the nonreciprocal magnon decay in a similar way.

ACKNOWLEDGMENTS

We thank fruitful discussions with Alexander Mook, Sota Kitamura, Shun Okumura, Joji Nasu, Shinnosuke Koyama, Hosho Kastura. T.M. was supported by JSPS KAKENHI Grant 23H01119, 23K17665 (T.M.), and JST CREST (Grant No. JPMJCR19T3) (T.M.). K.F. was supported by the Forefront Physics and Mathematics program to drive transformation (FoPM).

Appendix A: Magnon-magnon interactions for ferromagnetic Heisenberg model

We present an expression for the cubic Hamiltonian H_3 in Eq. (3c). In the ferromagnetic Heisenberg model on the honeycomb model defined by Eq. (10), H_3 is introduced by the in-plane DM interaction and the nonzero components of $V^{abc}_{\boldsymbol{k},\boldsymbol{q},\boldsymbol{p}}$ in Eq.(3c) are

$$V^{1,2,1}_{\boldsymbol{k},\boldsymbol{q},\boldsymbol{p}} = -D\sqrt{\frac{S}{2}}\sum_{j=1}^{3} e^{i\phi_{\delta_j} - i\boldsymbol{q}\cdot\boldsymbol{\delta}_j}, \tag{A1a}$$

$$V^{1,2,2}_{\boldsymbol{k},\boldsymbol{q},\boldsymbol{p}} = D\sqrt{\frac{S}{2}}\sum_{j=1}^{3} e^{i\phi_{\delta_j} + i\boldsymbol{k}\cdot\boldsymbol{\delta}_j}, \tag{A1b}$$

$$V^{2,1,1}_{\boldsymbol{k},\boldsymbol{q},\boldsymbol{p}} = -D\sqrt{\frac{S}{2}}\sum_{j=1}^{3} e^{i\phi_{\delta_j} - i\boldsymbol{k}\cdot\boldsymbol{\delta}_j}, \tag{A1c}$$

$$V^{2,1,2}_{\boldsymbol{k},\boldsymbol{q},\boldsymbol{p}} = -D\sqrt{\frac{S}{2}}\sum_{j=1}^{3} e^{i\phi_{\delta_j} + i\boldsymbol{q}\cdot\boldsymbol{\delta}_j}, \tag{A1d}$$

where $\phi_{\delta_j} = \arg(\boldsymbol{d}^y_{\delta_j} - i\boldsymbol{d}^x_{\delta_j})$ and $\boldsymbol{d}_{\delta_j}$ is the direction of the DM interaction on the bond $\boldsymbol{\delta}_j$ written as

$$\boldsymbol{d}_{\delta_1} = (0, 1), \tag{A2a}$$

$$\boldsymbol{d}_{\delta_2} = (-\frac{\sqrt{3}}{2}, -\frac{1}{2}), \tag{A2b}$$

$$\boldsymbol{d}_{\delta_3} = (\frac{\sqrt{3}}{2}, -\frac{1}{2}). \tag{A2c}$$

Appendix B: The "explicitly broken TRS" model

We consider the order of the magnitude of the nonlinear thermal responses of a system with "explicitly broken TRS". We write the Hamiltonian of this model as H_z which is the Hamiltonian (10) with the modification $\boldsymbol{d}_{ij} = (0, 0, D)$ for the next-nearest neighbor bond for A sites and $\boldsymbol{d}_{ij} = (0, 0, -D)$ for the next-nearest neighbor bond for B sites. In this model, because of the broken effective TRS and inversion symmetry, the nonlinear Drude term can be nonzero within the harmonic theory with H_2. This model also has the C_3 rotation symmetry and the symmetry IM_x composed of inversion symmetry and mirror symmetry along the yz-plane. Thus, we have $\sigma^{yyy} = -\sigma^{yxx}$ and $\sigma^{xxx} = \sigma^{xyy} = 0$. We assume that the magnon lifetime is determined by the phenomenological damping α as $\tau_{\boldsymbol{k}} = 1/2\alpha\varepsilon_{\boldsymbol{k}}$ and we obtain the nonlinear conductivity $\sigma^{\mu\nu\nu}$ for the "explicitly broken TRS" model as shown in Fig. 5 by using the same parameters as Fig. 4(a). By using the peak value of the $\sigma^{\mu\nu\nu}$,

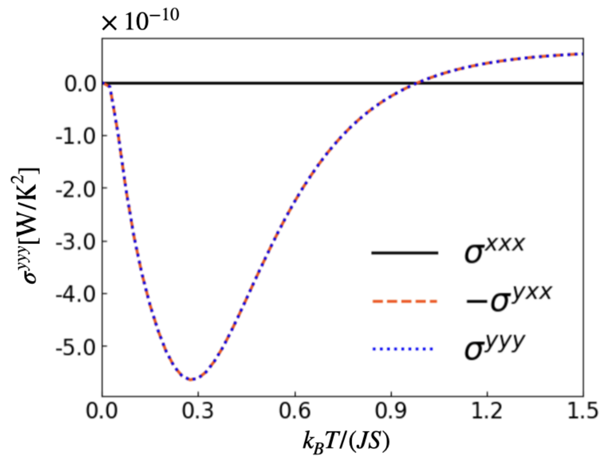

FIG. 5. Temperature dependence of $\sigma^{\mu\nu\nu}$ calculated with the "explicitly broken TRS" model H_z. We used the following parameters: $D/J = 0.15$, $\Delta_A = 0.0$, $\Delta_B = 0.05$, $h/J = 0.1$, $\mu_A = \mu_B = 1.0$, $S = 1$ and $\alpha = 0.001$.

we assume that the order of $\sigma^{\mu\nu\nu}$ is 10^{-10} W/K^2 which is the same order of the nonlinear thermal conductivity induced by the magnon-magnon interaction. Thus, the magnon-magnon interaction is comparable to the "explicitly broken TRS" of the free magnon Hamiltonian.

[1] A. V. Chumak, V. Vasyuchka, A. Serga, and B. Hillebrands, Nature Physics **11**, 453 (2015).
[2] H. Katsura, N. Nagaosa, and P. A. Lee, Physical Review Letters **104**, 066403 (2010).
[3] Y. Onose, T. Ideue, H. Katsura, Y. Shiomi, N. Nagaosa, and Y. Tokura, Science **329**, 297 (2010).
[4] J. Xiao, G. E. W. Bauer, K.-c. Uchida, E. Saitoh, and S. Maekawa, Physical Review B **81**, 214418 (2010).
[5] R. Matsumoto and S. Murakami, Physical Review Letters **106**, 197202 (2011).
[6] R. Cheng, S. Okamoto, and D. Xiao, Physical Review Letters **117**, 217202 (2016).
[7] V. A. Zyuzin and A. A. Kovalev, Physical Review Letters **117**, 217203 (2016).
[8] R. Takashima, Y. Shiomi, and Y. Motome, Physical Review B **98**, 020401 (2018).
[9] H. Kondo and Y. Akagi, Physical Review Research **4**, 013186 (2022).
[10] I. Proskurin, A. S. Ovchinnikov, J.-i. Kishine, and R. L. Stamps, Physical Review B **98**, 134422 (2018).
[11] H. Ishizuka and M. Sato, Physical Review B **100**, 224411 (2019).
[12] H. Ishizuka and M. Sato, Physical Review Letters **129**, 107201 (2022).
[13] K. Fujiwara, S. Kitamura, and T. Morimoto, arXiv preprint arXiv:2210.17099 (2022).
[14] A. Sekine and N. Nagaosa, Physical Review B **101**, 155204 (2020).
[15] H. Varshney, R. Mukherjee, A. Kundu, and A. Agarwal, Physical Review B **108**, 165412 (2023).
[16] R. Mukherjee, S. Verma, and A. Kundu, Physical Review B **107**, 245426 (2023).
[17] R. J. Elliott and M. F. Thorpe, Journal of Physics C: Solid State Physics **2**, 312 (1969).
[18] A. B. Harris, D. Kumar, B. I. Halperin, and P. C. Hohenberg, Physical Review B **3**, 961 (1971).
[19] M. E. Zhitomirsky and A. L. Chernyshev, Physical Review Letters **82**, 4536 (1999).
[20] R. Costa Filho, M. Cottam, and G. Farias, Physical Review B **62**, 6545 (2000).
[21] A. L. Chernyshev and M. E. Zhitomirsky, Physical Review Letters **97**, 207202 (2006).
[22] A. L. Chernyshev and M. E. Zhitomirsky, Physical Review B **79**, 144416 (2009).
[23] M. Mourigal, M. E. Zhitomirsky, and A. L. Chernyshev, Physical Review B **82**, 144402 (2010).
[24] M. Mourigal, W. T. Fuhrman, A. L. Chernyshev, and M. E. Zhitomirsky, Physical Review B **88**, 094407 (2013).
[25] M. E. Zhitomirsky and A. L. Chernyshev, Reviews of Modern Physics **85**, 219 (2013).
[26] A. Chernyshev and P. Maksimov, Physical Review Letters **117**, 187203 (2016).
[27] P. A. Maksimov, M. E. Zhitomirsky, and A. L. Chernyshev, Physical Review B **94**, 140407 (2016).
[28] P. A. Maksimov and A. L. Chernyshev, Physical Review B **93**, 014418 (2016).
[29] S. M. Winter, K. Riedl, P. A. Maksimov, A. L. Chernyshev, A. Honecker, and R. Valentí, Nature Communications **8**, 1152 (2017).
[30] S. S. Pershoguba, S. Banerjee, J. Lashley, J. Park, H. Ågren, G. Aeppli, and A. V. Balatsky, Physical Review X **8**, 011010 (2018).
[31] P. A. McClarty, X.-Y. Dong, M. Gohlke, J. G. Rau, F. Pollmann, R. Moessner, and K. Penc, Physical Review B **98**, 060404 (2018).
[32] J. G. Rau, R. Moessner, and P. A. McClarty, Physical Review B **100**, 104423 (2019).

[33] P. A. Maksimov and A. L. Chernyshev, Physical Review Research **2**, 033011 (2020).
[34] A. Mook, J. Klinovaja, and D. Loss, Physical Review Research **2**, 033491 (2020).
[35] R. L. Smit, S. Keupert, O. Tsyplyatyev, P. A. Maksimov, A. L. Chernyshev, and P. Kopietz, Physical Review B **101**, 054424 (2020).
[36] A. Mook, K. Plekhanov, J. Klinovaja, and D. Loss, Physical Review X **11**, 021061 (2021).
[37] Y.-S. Lu, J.-L. Li, and C.-T. Wu, Physical Review Letters **127**, 217202 (2021).
[38] P. A. Maksimov and A. L. Chernyshev, Physical Review B **106**, 214411 (2022).
[39] H. Sun, D. Bhowmick, B. Yang, and P. Sengupta, Physical Review B **107**, 134426 (2023).
[40] S. Koyama and J. Nasu, Physical Review B **108**, 235162 (2023).
[41] Q.-H. Chen, F.-J. Huang, and Y.-P. Fu, Physical Review B **108**, 024409 (2023).
[42] N. Heinsdorf, D. G. Joshi, H. Katsura, and A. P. Schnyder, arXiv preprint arXiv:2309.15113 (2023).
[43] J. Habel, A. Mook, J. Willsher, and J. Knolle, Physical Review B **109**, 024441 (2024).
[44] K. Sourounis and A. Manchon, arXiv preprint arXiv:2402.14572 (2024).
[45] S. Koyama and J. Nasu, arXiv preprint arXiv:2403.08478 (2024).
[46] W. B. Yelon and R. Silberglitt, Physical Review B **4**, 2280 (1971).
[47] L. Chen, J.-H. Chung, B. Gao, T. Chen, M. B. Stone, A. I. Kolesnikov, Q. Huang, and P. Dai, Physical Review X **8**, 041028 (2018).
[48] K. S. Burch, D. Mandrus, and J.-G. Park, Nature **563**, 47 (2018).
[49] W. Xing, L. Qiu, X. Wang, Y. Yao, Y. Ma, R. Cai, S. Jia, X. Xie, and W. Han, Physical Review X **9**, 011026 (2019).
[50] B. Yuan, I. Khait, G.-J. Shu, F. Chou, M. Stone, J. Clancy, A. Paramekanti, and Y.-J. Kim, Physical Review X **10**, 011062 (2020).
[51] H. Zhang, C. Xu, C. Carnahan, M. Sretenovic, N. Suri, D. Xiao, and X. Ke, Physical Review Letters **127**, 247202 (2021).
[52] P. Czajka, T. Gao, M. Hirschberger, P. Lampen-Kelley, A. Banerjee, N. Quirk, D. G. Mandrus, S. E. Nagler, and N. P. Ong, Nature Materials **22**, 36 (2023).
[53] T. Holstein and H. Primakoff, Physical Review **58**, 1098 (1940).
[54] I. Sodemann and L. Fu, Physical Review Letters **115**, 216806 (2015).
[55] T. Ideue, Y. Onose, H. Katsura, Y. Shiomi, S. Ishiwata, N. Nagaosa, and Y. Tokura, Physical Review B **85**, 134411 (2012).
[56] M. Hirschberger, R. Chisnell, Y. S. Lee, and N. Ong, Physical Review Letters **115**, 106603 (2015).
[57] S. Park, N. Nagaosa, and B.-J. Yang, Nano Letters **20**, 2741 (2020).
[58] C. Xu, J. Feng, H. Xiang, and L. Bellaiche, npj Computational Materials **4**, 57 (2018).
[59] I. Lee, F. G. Utermohlen, D. Weber, K. Hwang, C. Zhang, J. van Tol, J. E. Goldberger, N. Trivedi, and P. C. Hammel, Physical Review Letters **124**, 017201 (2020).
[60] K. Nakazawa, Y. Kato, and Y. Motome, Physical Review B **105**, 165152 (2022).
[61] Y. Shiomi, R. Takashima, and E. Saitoh, Physical Review B **96**, 134425 (2017).
[62] T. Ideue, T. Kurumaji, S. Ishiwata, and Y. Tokura, Nature Materials **16**, 797 (2017).